The flow boiling heat transfer coefficient determination in a minichannel used the FEM combined with Trefftz functions

Magdalena Piasecka[1*], *Kinga* Strąk[2], and *Beata* Maciejewska[3]

[1,2] Faculty of Mechatronics and Mechanical Engineering
[3] Faculty of Management and Computer Modelling
Kielce University of Technology, Al. 1000-lecia P.P. 7, 25-314 Kielce, Poland

Abstract. The method of solving the inverse heat conduction problem, by means of the FEM with Trefftz-type basis functions, during flow boiling in a minichannel was shown. This basis functions were constructed with using the Hermite interpolation and Trefftz functions. The aim of the numerical calculations was to determine the local heat transfer coefficient on the basis of experimental data in a horizontally oriented minichannel. The refrigerant flowing along the minichannel (HFE-649 or HFE-7100) was heated by a thin enhanced plate by vibration-assisted laser texturing. The temperature on an outer smooth side of the plate was detected by means of infrared thermography. On the heated wall–fluid contact surface in the minichannel the heat transfer coefficient was obtained from the Robin boundary condition. It was assumed that the temperature distribution in the heated plate was described by the Poisson equation. The unknown values of temperature and temperature derivatives at nodes were computed by minimizing the functional which describes the mean square error of the approximate solution on the boundary and along common edges of neighbouring elements. The results were presented as the heated plate temperature and heat transfer coefficient versus the minichannel length.

1 Introduction

Heat transfer in small channels has been investigated intensively over the past years, particularly for application as cooling electronic components. Due to change of the state during the flow boiling in small channels, it is possible to meet opposing needs at the same time, i.e. receipt a heat flux as large as likely at small temperature difference between the heating surface and the saturated liquid. It is known from the literature that many factors influence flow boiling heat transfer in minichannels. One of them is using boiling liquids of different physical properties.

Ramakrishnan et al. [1] performed the pool boiling using HFE-649 and HFE-7100 fluids in microporous and microfinned heat sinks. Enhanced heat sinks performed better than bare die in experiments using HFE-649 and HFE-7100 under subcooled conditions. Konishi et al. [2] presented a study to FC-72 flow boiling CHF mechanisms encountered at different orientations relative to Earth's gravity when the fluid is supplied as a two-phase mixture. Mancin et al. [3] discussed the effects of various parameters on the single-phase liquid and flow boiling of R134a and R1234ze (E) inside a 5 pores per linear inch copper foam. Dutkowski [4] presented studies on boiling of the refrigerant R134a in minichannels. Mikielewicz et al. [5] performed flow boiling heat transfer and flow condensation for data collected from literature for such fluids as R404a, R600a, R290, R32, R134a, R1234yf and other. Bohdal et al. [6] conducted the investigation of flow structures during HFE-7100 refrigerant condensation in pipe minichannels.

The data from the experiments using several refrigerants were the basis for the analysis of steady-state flow boiling heat transfer in minichannels with smooth and enhanced heated surface performed by the authors of this paper in their previous works [7–10].

The numerical calculations involves determining the heat transfer coefficient by solving the boundary inverse heat conduction problem [11] using the FEM with the Trefftz functions and the Hermite interpolation [12]. These functions exactly satisfying the governing equation and are suitable for solving both direct and inverse problems. More information on the Trefftz function can be found in [13–18].

2 Experiment

The test section with a single rectangular minichannel (1, Fig. 1, Fig. 2) is the essential part of the main flow loop at the experimental stand shown in Fig. 1.

The refrigerant (HFE-649 or HFE-7100, 3M) flowing along the minichannel was heated by a thin plate enhanced by vibration-assisted laser texturing in contact with the fluid. Infrared thermography was used to determine changes in the temperature on the outer smooth side of the plate. The other side of the channel

*Corresponding author: tmpmj@tu.kielce.pl

with a glass panel allowed observing the vapour-liquid flow patterns on the enhanced heated plate side. K-type thermocouples and pressure meters were installed in the inlet and outlet of the minichannel. The research equipment comprised: a data and image acquisition system with digital cameras, a computer with special software, a lighting system and the power supply system.

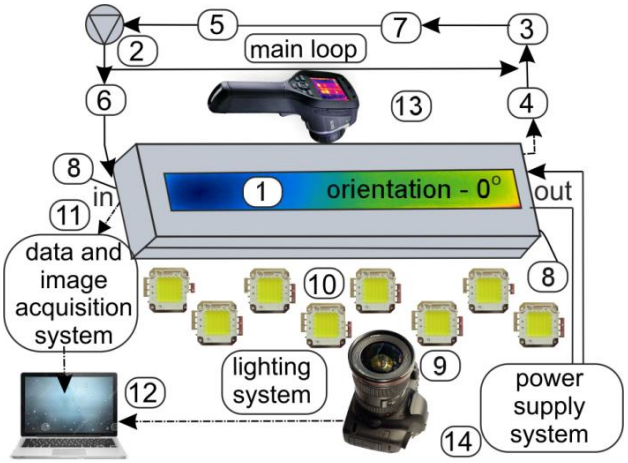

Fig. 1. The schematic diagram of the main systems of the experimental setup, 1- a test section with a minichannel, 2 -a gear pump, 3 - a compensating tank/a pressure regulator, 4 - a tube-type heat exchanger, 5 - a filter, 6 - a mass flowmeter, 7 - a deaerator, 8 - a pressure converter, 9 - a quick shot camera, 10 - a high power LEDs, 11 - a data acquisition station, 12 - a PC, 13 - an infrared camera, 14 - a power supply system.

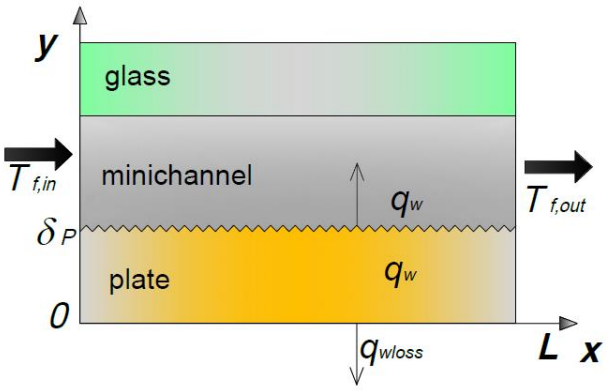

Fig. 2. Schematic diagram of the main elements of the test section with a minichannel.

3 Analysis and modelling

The aim of the numerical calculations, based on an experimental data, was to determine the heat transfer coefficient during FC-72 flow boiling in a minichannel from the Robin boundary condition:

$$h(x)=\frac{-\lambda_P \dfrac{\partial T_P(x,\delta_P)}{\partial y}}{T_P(x,\delta_P)-T_f(x)} \tag{1}$$

where λ_P – the thermal conductivity coefficient of the plate, δ_P – the plate thickness, T_P – the plate temperature, T_f –the fluid temperature calculated from the assumption of the linear dependence between the the fluid inlet temperature and the fluid outlet temperature in the minichannel, x – the spatial variable related to the flow direction, y – the spatial variable referred to the perpendicular direction to the flow direction and associated with the plate thickness (see Fig. 2).

The plate temperature was the solution of the inverse two-dimensional heat conduction problem in the plate. The plate temperature was described by Poisson's equation:

$$\nabla^2 T_P = -\frac{q_w}{\delta_P \cdot \lambda_P} \text{ for } (x,y)\in\Omega_P, \tag{2}$$

The boundary conditions have the form:

$$T_P(x_k,0)=T_k \text{ for } k=1,2,\ldots,K \tag{3}$$

$$\frac{\partial T_P}{\partial x}(0,y)=0, \tag{4}$$

$$\frac{\partial T_P}{\partial x}(L,y)=0, \tag{5}$$

$$\lambda_P \frac{\partial T_P}{\partial y}(x,0)=q_{wloss}, \tag{6}$$

where heat flux is defined as $q_w=\dfrac{I\cdot\Delta U}{A}$, I – current intensity, ΔU – the voltage drop accross the plate, A – the surface area of the plate, $\Omega_P=\left\{(x,y)\in R^2 : 0<x<L,\ \ 0<y<\delta_P\right\}$, L – the length of a minichannel, K – the number of measurements, T_k – the plate temperature measured by infrared thermography at the boundary $y=0$, q_{wloss} – the heat loss to the surroundings, λ_P, δ_P – defined as for Eq. (1).

The solution method for Eq. (2) is a generalisation of the approach shown in [19] regarding to the one-dimensional heat conduction equation and using the Lagrange interpolation.

The inverse problem (Eqs. 2-6) in the heated plate Ω_P divided into elements Ω_P^j was solved by the FEM with Trefftz-type basis functions $f_{jk}(x,y)$, $g_{jk}(x,y)$, $h_{jk}(x,y)$ based on the Hermite interpolation [20], where j – the element number, k– the basis function number in the j-th element.

The basis functions $f_{jk}(x,y)$, $g_{jk}(x,y)$, $h_{jk}(x,y)$ are a linear combinations of Trefftz functions and they have the following properties in nodes (x_i,y_i)

$$f_{jk}(x_i,y_i)=\delta_{ki},\ \frac{\partial f_{jk}}{\partial x}(x_i,y_i)=0,\ \frac{\partial f_{jk}}{\partial y}(x_i,y_i)=0$$

$$g_{jk}(x_i, y_i) = 0\,,\ \frac{\partial g_{jk}}{\partial x}(x_i, y_i) = \delta_{ki}\,,\ \frac{\partial g_{jk}}{\partial y}(x_i, y_i) = 0\,,$$

$$h_{jk}(x_i, y_i) = 0\,,\ \frac{\partial h_{jk}}{\partial x}(x_i, y_i) = 0\,,\ \frac{\partial h_{jk}}{\partial y}(x_i, y_i) = \delta_{ki}\,,$$

$$i = 1,2,\ldots, N \qquad (7)$$

where j – the element number, k– the basis function number in the j-th element, N – number of nodes in the j-th element.

The plate temperature in each element Ω_P^j is approximated by a linear combination of Trefftz-type basis functions and has the form:

$$T_P^j(x,y) = u(x,y) + \sum_{k=1}^{N}\Big((a_n - u(x_n,y_n))\,f_{jk}(x,y) + \big(b_n - u'_x(x_n,y_n)\big)g_{jk}(x,y) + \big(c_n - u'_y(x_n,y_n)\big)h_{jk}(x,y)\Big)\,, \qquad (8)$$

where n is the node number in the whole domain Ω_P, $u(x,y)$ – particular solution of equation Eq. (2), a_n – value of the unknown temperature function at the n-th node of the domain Ω_P, b_n –value of the partial derivative of the unknown temperature function with respect to x at the n-th node of the domain Ω_P, c_n – value of the partial derivative of the unknown temperature function with respect to y at the n-th node of the domain Ω_P, j, k, N – defined as for Eq. (7).

The unknown coefficients a_n, b_n, c_n of linear combination of Eq. (8) were calculated, as in [21], by minimizing the functional whichdescribes the mean square error of the approximate solution at the domain boundaries and along common edges of neighboring elements.

4 Results and discussion

The analysis includes the data from the experiments performed using two refrigerants: HFE-649 and HFE-7100. The experiments were recorded for two heat fluxes supplied to the heated plate under similar stable thermal and flow conditions (at a stationary condition).

Experimental parameters are presented in Table 1.

The results are presented as:

- the heated plate temperature measured by infrared thermography and the distance from the minichannel inlet - Fig. 3,
- the heat transfer coefficient and the distance from the minichannel inlet - Fig. 4,

for two selected values of heat flux: 48 and 65 kW/m^2.

The study focused on heat transfer coefficient identification only in the region of subcooled boiling. The coefficient values were determined by solving the inverse heat conduction problem using the FEM with Trefftz-type basis functions based on the Hermite interpolation. The results obtained on the basis of heated surface temperatures at the inlet and outlet of the minichannel (about 10% from each side) were ignored due to the occurrence of the largest measurement errors when using infrared thermography, as reported in [22].

Table 1. Experimental parameters.

Heat flux density q_w kW/m^2	**Average mass flux G kg /(m^2·s)**	**Average inlet pressure p_{in} kPa**	**Average inlet liquid sub-cooling ΔT_{sub} K**
48	361	108	45
65	428	145	52

Analysis of temperature distributions on the heated surface, shown in Fig. 3, indicated the highest plate temperatures were achieved for HFE-7100 fluid and for the highest heat flux (65 kW/m^2) from 0.08 m to 0.16 m distance from the minichannel inlet, Fig. 3b. For lower heat flux (48 kW/m^2), the highest temperature distribution was obtained for HFE-649 fluid (Fig. 3a) at all distance of the minichannel length. For higher heat fluxes was obtained the highest temperature distributions for both fluids.

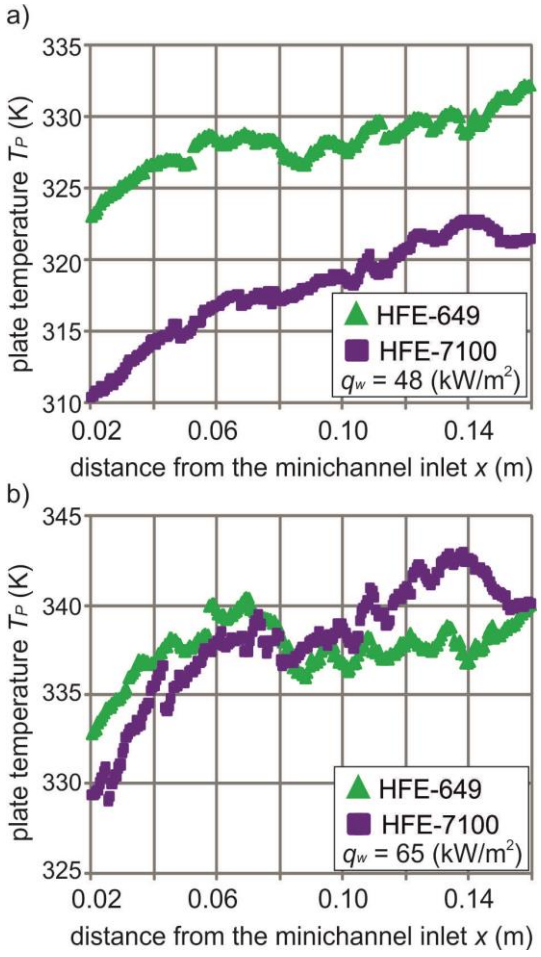

Fig.3. The plate temperature vs. the minichannel length, a) q_w = 48 kW/m^2, b) q_w = 65 kW/m^2; experimental parameters are shown in Table 1.

In the subcooled boiling region heat transfer coefficient values were in the range 1.7 kW/(m^2·K) to 2.6 kW/(m^2·K) for two selected values of the heat flux, Fig. 4. The highest values of the heat transfer coefficient were recorded for HFE-7100 fluid at lower heat flux (48 kW/m^2), Fig. 4a.·It was also observed that for heat flux of 65 kW/m^2 higher values of the heat transfer coefficient were recorded for HFE-649 fluid at the distance from 0.05 m from the minichannel inlet to its outlet, Fig. 4b.·The heat transfer values of coefficients calculated for both fluids slightly fluctuated with the distance from the minichannel inlet.

It can be noticed that the coefficient values were relatively low in comparison to those at the saturated boiling region, discussed in [7,23,24].

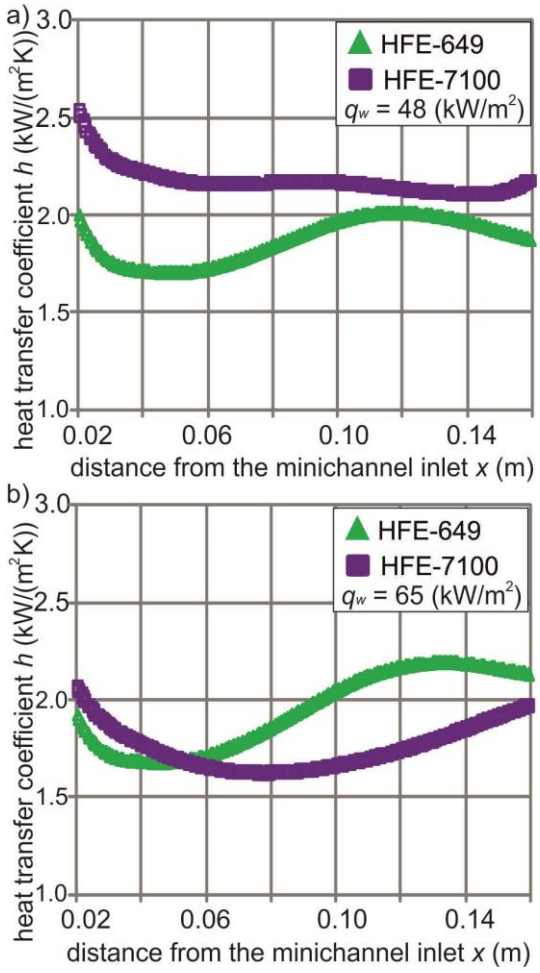

Fig. 4. The heat transfer coefficient vs. the minichannel length, at the subcooled boiling region, a) q_w = 48 kW/m^2, b) q_w = 65 kW/m^2; experimental parameters are shown in Table 1.

5 Conclusions

In this results of flow boiling heat transfer in a minichannel at subcooled boiling region were shown. During experiments two refrigerants (HFE-649 or HFE-7100, 3M) flowing in a single minichannel were heated by a thin enhanced plate. Infrared thermography was used to determine changes in the temperature on its outer side. The method of solving the inverse heat conduction problem by means of the FEM with Trefftz-type basis functions was proposed. This basis functions were constructed with using the Hermite interpolation and Trefftz functions. The heat transfer coefficient, on the heated wall–fluid contact surface in the minichannel, was obtained from the Robin boundary condition. The numerical calculations were performed in the subcooled boiling region. The results were presented as the heated plate temperature and heat transfer coefficient versus the channel length. The calculated heat transfer coefficient values were in the range 1.7 to 2.6 kW/(m^2·K). The highest values of the heat transfer coefficient were recorded for HFE-7100 fluid at lower heat flux.·The heat transfer coefficients calculated for both fluids slightly fluctuated with the distance from the minichannel inlet.

References

1. B. Ramakrishnan,S. H. Bhavnani, J. Gess, R. W. Knight, D. Harris, R. W. Johnson, IEEE Semicond. Therm. Meas. Manag. Symp. 6892210 (2014)
2. C. Konishi, I. Mudawar,M. M. Hasan, Int. J. Heat Mass Transf., **65** (2013)
3. S. Mancin, A. Diani, L. Doretti, L. Rossetto, Int. J. Heat Mass Transf., **74** (2014)
4. K. Dutkowski, Int. J. Heat Mass Transf. **53**, 5–6 (2010)
5. D. Mikielewicz, R. Andrzejczyk, B. Jakubowska, J. Mikielewicz, Arch. Thermodyn. **35**, 3 (2014)
6. T. Bohdal, M. Sikora, K. Widomska, A. M. Radchenko, Arch. Thermodyn. **36**, 4 (2015)
7. B. Maciejewska, K. Strąk, M. Piasecka, Procedia Eng., **157** (2016)
8. K. Strąk,M. Piasecka, B. Maciejewska, Int. J. Heat Mass Transf., **117** (2018)
9. M. Piasecka, Metrol. Meas. Sys. **XX**, (2) 205–216 (2013)
10. M. Piasecka, K. Strąk, B. Maciejewska, Heat Transf. Eng. **38**, 3 (2017)
11. J. V. Beck, B. Blackwell, Jr., C. R. St. Clair, *Inverse Heat Conduction* (Wiley – Interscience Publ., New York, 1985)
12. D. Kincaid, W. Cheney, *Numerical Analysis: Mathematics of Scientific Computing* (3rd Ed., Brooks/Cole Publishing Company, Belmont, California, 2002)
13. I. Herrera, Numer. Methods Partial Differ. Equ. **16**, 6 (2000)
14. A. Maciąg, J. Theor. Appl. Mech. **49**, 1 (2011)
15. K. Grysa, B. Maciejewska, J. Theor. Appl. Mech. **51**, 2 (2013)
16. S. Hozejowska, R. Kaniowski, M. E. Poniewski, Int. J. Numer. Methods Heat Fluid Flow **24**, 4 (2014)
17. B. Maciejewska, K. Strak, M. Piasecka, Int. J. Numer. Methods Heat Fluid Flow **28**, 1 (2018)

18. B. Maciejewska, M. Piasecka, Int. J. Heat Mass Transf., **107** (2017)
19. M. Cialkowski, J. Therm. Sci. **11**, 2 (2002)
20. B. Maciejewska, J. Theor. Appl. Mech. **55**, 1 (2017)
21. B. Maciejewska, M. Piasecka, Heat Mass Transf. **53**, 4 (2017)
22. D. Michalski, K. Strak, M. Piasecka, EPJ Web Conf. **143**, 02075 (2017)
23. M. Piasecka, K. Strąk, B. Grabas, Arch. Metall. Mater. **62**, 4 (2017)
24. M. Piasecka, K. Strąk, B. Maciejewska, B. Grabas, J. Phys. Conf. Ser. **745**, 032123 (2016)